

Carbon and Chlorine Isotope Fractionation Patterns Associated with Different Engineered Chloroform Transformation Reactions

Clara Torrentó,^{*,†,‡,§} Jordi Palau,^{†,‡,§} Diana Rodríguez-Fernández,^{‡,§} Benjamin Heckel,[§] Armin Meyer,[§] Cristina Domènech,[‡] Mònica Rosell,[‡] Albert Soler,[‡] Martin Elsner,^{§,⊥} and Daniel Hunkeler[†]

[†]Centre for Hydrogeology and Geothermics, Université de Neuchâtel, 2000 Neuchâtel, Switzerland

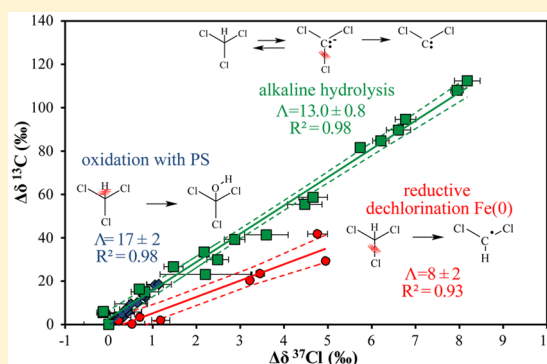
[‡]Grup de Mineralogia Aplicada i Geoquímica de Fluids, Departament de Mineralogia, Petrologia i Geologia Aplicada, Facultat de Ciències de la Terra, Martí Franques s/n, Universitat de Barcelona (UB), 08028 Barcelona, Spain

[§]Institute of Groundwater Ecology, Helmholtz Zentrum München, 85764 Neuherberg, Germany

[⊥]Chair of Analytical Chemistry and Water Chemistry, Technical University of Munich, Marchioninistrasse 17, D-81377 Munich, Germany

Supporting Information

ABSTRACT: To use compound-specific isotope analysis for confidently assessing organic contaminant attenuation in the environment, isotope fractionation patterns associated with different transformation mechanisms must first be explored in laboratory experiments. To deliver this information for the common groundwater contaminant chloroform (CF), this study investigated for the first time both carbon and chlorine isotope fractionation for three different engineered reactions: oxidative C–H bond cleavage using heat-activated persulfate, transformation under alkaline conditions (pH ~ 12) and reductive C–Cl bond cleavage by cast zerovalent iron, Fe(0). Carbon and chlorine isotope fractionation values were $-8 \pm 1\%$ and $-0.44 \pm 0.06\%$ for oxidation, $-57 \pm 5\%$ and $-4.4 \pm 0.4\%$ for alkaline hydrolysis (pH 11.84 \pm 0.03), and $-33 \pm 11\%$ and $-3 \pm 1\%$ for dechlorination, respectively. Carbon and chlorine apparent kinetic isotope effects (AKIEs) were in general agreement with expected mechanisms (C–H bond cleavage in oxidation by persulfate, C–Cl bond cleavage in Fe(0)-mediated reductive dechlorination and E1_{CB} elimination mechanism during alkaline hydrolysis) where a secondary AKIE_{Cl} (1.00045 ± 0.00004) was observed for oxidation. The different dual carbon-chlorine ($\Delta\delta^{13}\text{C}$ vs $\Delta\delta^{37}\text{Cl}$) isotope patterns for oxidation by thermally activated persulfate and alkaline hydrolysis (17 ± 2 and 13.0 ± 0.8 , respectively) vs reductive dechlorination by Fe(0) (8 ± 2) establish a base to identify and quantify these CF degradation mechanisms in the field.



1. INTRODUCTION

Chloroform (CF) is both an anthropogenic environmental contaminant widely distributed around the world as well as a natural compound formed in various aquatic and terrestrial environments.^{1–3} CF of anthropogenic origin has been extensively used as degreasing agent and as a precursor to Teflon and various refrigerants and was historically used in medicine as anesthetic. It is formed as oxidation byproduct during drinking water treatment⁴ and may form as a daughter product of carbon tetrachloride (CT) dehalogenation at contaminated sites. As a result, CF is one of the most frequently detected volatile organic compounds (VOCs) in groundwater.⁵ Taking into account its high ecotoxicity,⁶ CF prominently ranks among the halogenated VOCs on the Agency for Toxic Substances and Disease Registry priority list of hazardous substances.⁷

Aerobic and anaerobic cometabolic biodegradation processes of CF have been described.⁸ However, CF cometabolic degradation is restricted by several environmental factors such

as the presence of other specific compounds that inhibit CF degradation, the availability of the substrate or the toxicity of derived metabolites.⁸ Reductive dechlorination of CF via dehalorespiration by two *Dehalobacter* sp. strains (CF50 and UNSWDHB) and one *Desulfitobacterium* sp. strain (PR) has recently been described in laboratory studies^{9–14} and proposed as anaerobic bioremediation strategy. However, this strategy is only applicable to contaminated sites in the absence of its parent compound, i.e. CT, which has been shown to strongly inhibit CF dehalorespiration in an enrichment culture containing *Dehalobacter* spp.¹⁵ In turn, CF itself is a strong inhibitor of chlorinated ethene- or ethane-degrading cultures even when present at low concentrations.^{16,17} These interdependencies make the remediation of sites contaminated with

Received: February 6, 2017

Revised: May 2, 2017

Accepted: May 9, 2017

Published: May 9, 2017

several chlorinated compounds particularly challenging so that multiple-stage remediation strategies are warranted in which inhibitors like chloromethanes are removed upfront.

Abiotic reactions bear potential to accomplish such an initial removal. Naturally occurring iron-bearing minerals like goethite and iron sulfide under low-redox environments have been demonstrated to be involved in the reductive dechlorination of CF.¹⁸ However, due to the very restricted natural attenuation conditions for CF and its complex distribution in the subsurface as a dense nonaqueous phase liquid (DNAPLs), more efficient engineered remediation strategies have been proposed to increase CF removal in the environment. As a result of the high oxidation state of carbon in CF, its degradation by in situ chemical oxidation (ISCO) is in general much less effective than for chlorinated ethenes using common oxidants such as permanganate, iron-activated persulfate (PS), ozone, hydrogen peroxide, or Fenton's Reagent.¹⁹ However, thermally activated PS was recently shown to be a better option for efficient CF oxidation with the advantage that under thermal activation, the strongly oxidizing sulfate radical and other reactive intermediates (i.e., hydroxyl radicals, or reducing radicals such as superoxide radicals, $O_2^{\bullet-}$) can be generated at neutral pH.^{20–23}

Alternatively, CF alkaline hydrolysis has recently been proposed as a remediation technology based on its occurrence in drainage trenches filled with concrete-based construction wastes.²⁴ For the sustainable use of this new remediation strategy, identifying and assessing the performance of CF degradation reaction by alkaline hydrolysis, as well as understanding the underlying mechanism, is important.

Finally, CF reductive dechlorination by zerovalent metals has been studied only at laboratory scale.^{25–29} Nevertheless, this remediation strategy has been successfully proven at field sites contaminated by chlorinated ethenes using permeable reactive barriers with micro/macro-scale Fe(0)^{30,31} or Fe(0) nanoparticle injection.^{32,33}

Improved methods are needed to delineate the relative efficacy of the above-mentioned CF remediation approaches in the field. During the last decades, compound-specific isotope analysis (CSIA) has evolved as a tool to monitor transformation reactions and to quantify the progress of natural and enhanced remediation of organic contaminants.^{34,35} Molecules with light isotopes in the reactive position typically react slightly faster than molecules containing the heavy ones leading to a kinetic isotope effect (KIE). As a consequence, the heavier isotopes (e.g., ^{13}C and ^{37}Cl) usually become enriched in the remaining substrate. For a given reaction, quantification of the extent of contaminant transformation based on stable isotope ratios requires the experimental determination of isotopic fractionation (ϵ , see [Materials and Methods](#)).³⁶

Isotopic fractionation values for transformation reactions need to be known for very practical reasons: (i) to understand what changes in isotope values can be expected in the field at all, and whether this holds promise to qualitatively detect degradation; (ii) to understand what mechanism lies behind the isotope effect, in order to subsequently choose an appropriate ϵ value for quantification in the field.

In order to gain insight into the underlying reaction mechanism, apparent kinetic isotope effects (AKIEs) can be derived from determined ϵ values taking into account which of the atoms in the target molecule are expected to be present at the reactive position. Comparison of the observed AKIEs to the theoretical maximum KIEs ("semiclassical Streitwieser Limits") associated with breakage of chemical bonds, enables

interpretation of occurring transition state(s) of a bond cleavage in terms of (i) primary isotope effects affecting the atoms present in the reacting bond, (ii) secondary isotope effects affecting atoms located adjacent to the reacting position.^{37,38} Often, however, it is uncertain whether additional factors exert an influence on observable isotope fractionation such as (iii) masking due to rate-limitation in mass transfer, and (iv) superimposed isotope effects of multiple reaction steps typical of enzyme catalysis or multistep chemical reactions.^{39–42} When observable isotope fractionation of a single element varies between experiments, it is, therefore, often uncertain whether this is due to a different mechanism, or whether these other factors are responsible. Dual-element isotope plots, that is, graphs in which changes in isotope values of one element are plotted against those of a second offer a more reliable distinction between reaction mechanisms than ϵ values alone.^{35,39,43–50}

Such information can be highly valuable in field situations. Nondestructive abiotic natural processes, such as sorption, volatilization or diffusion strongly affect concentrations of a contaminant, but generally do not cause significant isotopic fractionation.^{51–57} Temporal or spatial shifts in isotope ratios, in contrast, are highly indicative of degradation and can, therefore, better monitor the success of remediation strategies at contaminated sites than mass balances alone.⁵⁸ Dual (or multi) isotope patterns, finally, can even be used to derive the relative contribution of different reaction mechanisms and then to quantify the efficiency of each of them in the field—provided that ϵ values of these processes have previously been characterized in laboratory experiments.^{59–64}

Reported carbon isotope effects during CF transformation are, however, scarce in the literature. Chan et al.¹¹ reported a carbon isotope fractionation value of $-27.5 \pm 0.9\%$ during dehalorespiration of CF by a mixed culture containing *Dehalobacter* sp. strain CF50. In comparison, a much lower ϵ_C value of $-4.3 \pm 0.4\%$ was reported by Lee et al.²⁹ for the same dechlorination reaction by a mixed consortium containing another *Dehalobacter* sp. strain, UNSWDHB, whereas isotope fractionation in CF abiotic reductive dechlorination by microsized Fe(0) was found to be indistinguishable from that of the first experiment ($-29 \pm 2\%$). Significantly, larger carbon isotopic fractionation was observed for CF alkaline hydrolysis at pH ranging from 11.8 to 12.7 ($-53 \pm 3\%$).²⁴ To the best of our knowledge, chlorine isotope fractionation during any CF transformation mechanism has not been reported so far. Specifically, understanding whether different reaction mechanisms lead to characteristic patterns in dual C–Cl isotope plots is still limited even for chlorinated ethenes^{46,47,62} and, to our knowledge, is currently nonexistent for chlorinated methanes. Hence, there is a need to explore dual element CSIA for defined reactions under controlled laboratory conditions to pave the path for the interpretation of isotope data in field studies.

Therefore, the goal of this study was to determine carbon and, for the first time, chlorine isotope fractionation patterns for different transformation processes of CF in important abiotic engineered reactions in order to explore the ability of CSIA to identify these processes at field sites. The selected chemical reactions were: oxidative C–H bond cleavage by radicals produced from PS activation, alkaline hydrolysis of chloroform at pH 12 and C–Cl bond cleavage in reductive dechlorination by cast milli-sized Fe(0).

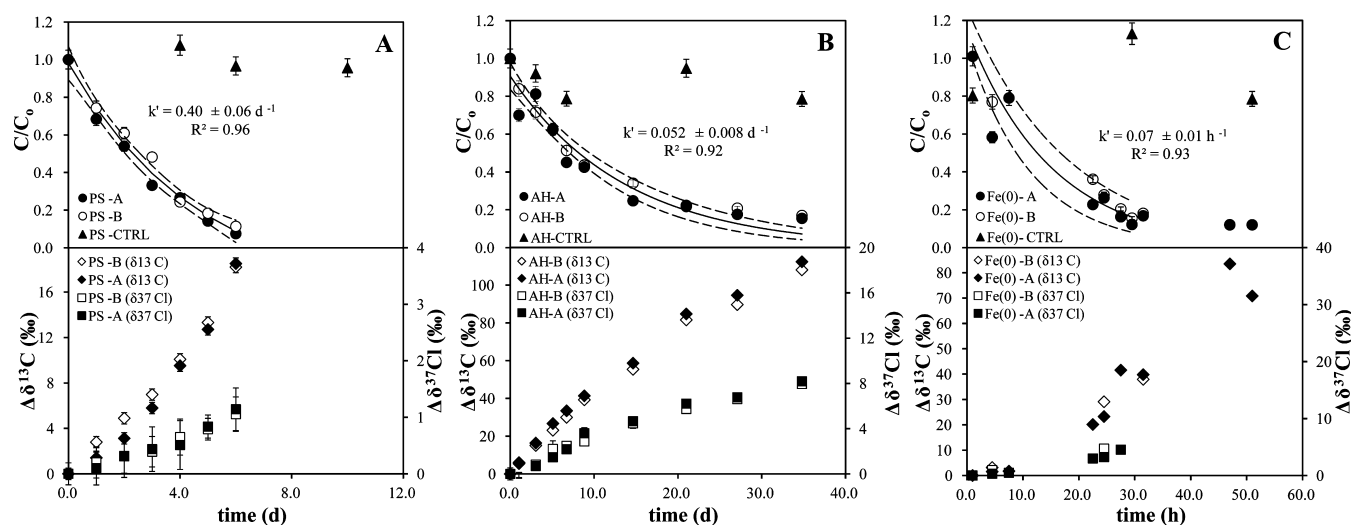


Figure 1. CF degradation kinetics (upper panels) and changes in C and Cl isotope ratios (lower panels) during oxidation by thermally activated PS with an initial PS/CF molar ratio of 40/1 (A), alkaline hydrolysis (B) and dechlorination by Fe(0) (C). Data from duplicate experiments (A and B parallel series) and from control (CTRL) experiments are shown. In the upper panels, the error bars show the uncertainty in C/C_0 , calculated by error propagation including uncertainty in concentration measurements. In some cases, error bars are smaller than the symbols. k' values were obtained from curve fittings according to eq SI4 (see Figure S1). Fits were conducted with linear regressions in Sigma Plot 10.0 for Windows. Dashed lines represent 95% CI of regression. For CF dechlorination with Fe(0), k' was calculated omitting data after 30 days when the disappearance of CF almost stopped. In the lower panels, error bars of individual data points indicate standard deviations of the measurements. In most cases, error bars are smaller than the symbols.

2. MATERIAL AND METHODS

2.1. Experimental Setup. All the experiments were conducted in duplicate using glass vials completely filled with aqueous solution without headspace to avoid partitioning of chlorinated volatile compounds into the gas phase. For the experiments with heat-activated PS and alkaline hydrolysis, 21 mL vials sealed with PTFE-coated rubber stoppers and aluminum crimp seals were used, whereas the Fe(0) experiments were performed using 42 mL clear glass vials capped with PTFE-coated rubber stoppers and plastic screw caps. A list of chemicals and additional experiment details is available in the Supporting Information (SI).

For the thermally activated PS experiments, the vials were filled with a pH 7 buffer solution and 0.5 mL of solutions with variable concentrations of PS were added to achieve initial PS-to-CF-molar ratios of 5/1, 10/1, or 40/1. The vials were placed in a thermostatic water bath at 50.0 ± 0.5 °C and the reaction was initiated by the addition of 0.5 mL of an aqueous CF (99%, Sigma-Aldrich) stock solution containing 2100 mg L^{-1} to achieve initial concentrations of 50 mg L^{-1} . The experiments lasted for 10 h and samples for analysis were collected at different time intervals. At each sampling time, the vials were removed from the water bath and immediately placed in an ice bath to quench the reaction by chilling. Samples were stored in the dark at 4 °C until analysis. Losses of CF due to volatilization and/or sorption were accounted for in control experiments set up in an identical manner except for the addition of PS.

CF alkaline hydrolysis experiments were performed at room temperature (~ 25 °C) in a pH 12 buffer solution and the vials were covered with aluminum foil to avoid photocatalyzed oxidation of CF. The reaction was initiated by the addition of 0.5 mL of the CF (99%, Sigma-Aldrich) stock solution to reach initial theoretical concentrations of 50 mg L^{-1} . The experiments started at different times to achieve reaction times varying from 0 to 35 days. After 35 days from the earliest prepared vials, all

the vials were sacrificed at the same time. An appropriate volume of 0.1 M acetic acid was added to the vials to neutralize the solution to pH 6 and quench the alkaline hydrolysis reaction. Samples were stored in the dark at 4 °C until analysis. Control experiments with unbuffered deionized water were also performed.

For the Fe(0) experiments, 2 g of milli-sized cast iron ($1.624 \pm 0.007 \text{ m}^2 \text{ g}^{-1}$) were added to each 42 mL vial to reach a surface concentration of $77 \text{ m}^2 \text{ L}^{-1}$. Afterward the vials were filled with a pH 6.6 buffer solution and the reaction was initiated by the addition of the CF pure phase (99%, Alfa Aesar) to reach initial theoretical concentrations of 100 mg L^{-1} . The vials were covered with aluminum foil to avoid photocatalyzed oxidation of CF and were rotated on a horizontal shaker (IKA KS 260 BASIC, Stanfen, Germany) at 200 rpm. Control experiments without iron were also carried out. The experiments were performed at room temperature (~ 25 °C) and they lasted 51 h. Reactions were stopped by filtration through $0.2 \mu\text{m}$ filters at different time intervals and samples for analysis were stored frozen in 10 mL vials covered with aluminum foil.

2.2. Analytical Methods. Detailed descriptions of analytical methods are available in the SI. Briefly, concentration measurements of chlorinated compounds were performed by headspace (HS) using GC/MS as explained elsewhere,²⁴ except for the samples from Fe(0) experiments for which GC/TOF/MS was used. Chloride anion concentrations were analyzed by high-performance liquid chromatography. Carbon isotope analyses of CF and some detectable volatile daughter products were performed using two different GC/IRMS systems located at the University of Neuchâtel (GC/IRMS-1)⁵⁰ and at the Scientific and Technological Centers of the University of Barcelona (GC/IRMS-2).²⁴ Chlorine isotope CF analyses were performed using a GC/qMS system from the University of Neuchâtel as explained elsewhere⁶⁶ or a GC/IRMS system from the Institute of Groundwater Ecology of the Helmholtz

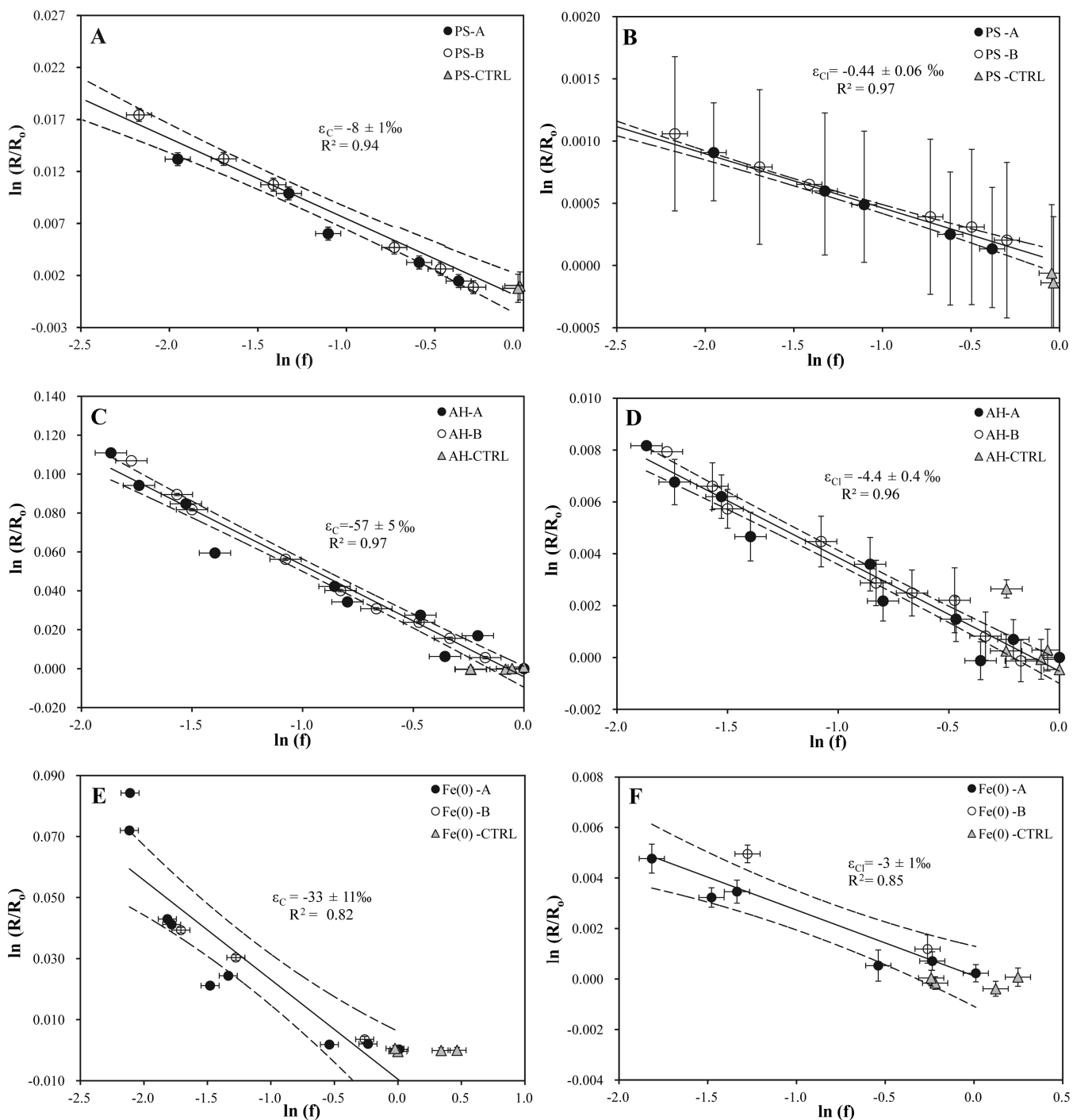


Figure 2. Logarithmic plots according to Rayleigh eq (eq 1) of carbon (left panels) and chlorine (right panels) isotope ratios during CF oxidation by thermally activated PS (A and B), alkaline hydrolysis (C and D) and dechlorination by Fe(0) (E and F). Data from duplicate experiments were used for estimating ϵ_C and ϵ_{Cl} . Dashed lines represent 95% CI of the linear regression. Error bars display the uncertainty calculated by error propagation including uncertainties in concentration and isotope measurements. In some cases, error bars are smaller than the symbols.

Zentrum München (GC/IRMS-3). An interlaboratory comparison demonstrating excellent agreement between the two analytical methods is provided in Heckel et al.⁶⁷

2.3. Isotope Data Evaluation. Bulk carbon and chlorine ϵ values were obtained from the slope of the linearized Rayleigh equation for a closed system:³⁶

$$\ln\left(\frac{\delta_t + 1}{\delta_0 + 1}\right) = \epsilon \times \ln f \tag{1}$$

where δ_0 and δ_t are isotope values in the beginning (0) and at a given time (t), respectively, and f is the fraction of substrate remaining at time t . Isotope signatures were reported in per mil (‰) using the delta notation relative to international standards, that is, Vienna PeeDee Belemnite for carbon ($\delta^{13}C_{VPDB}$) and the international Standard Mean Ocean Chloride (SMOC) for chlorine ($\delta^{37}Cl_{SMOC}$):

$$\delta(\text{in‰}) = (R/R_{std} - 1) \tag{2}$$

where R and R_{std} are the isotope ratios of the sample and the standard, respectively.

Errors given for ϵ values are the 95% confidence intervals (CI) of the slope of the regression line in the Rayleigh plots.

The apparent kinetic isotope effects (AKIEs) were calculated to evaluate the intrinsic isotope effect of the bond cleavage (see equations in the SI).

For dual C–Cl isotope plots, the slope of the correlation trend was determined by linear regression and the uncertainty corresponds to the 95% CI.

3. RESULTS AND DISCUSSION

3.1. Carbon and Chlorine Isotope Fractionation.

Changes in CF concentration and C and Cl isotope ratios of CF during degradation by the three different mechanisms are shown in Figure 1. No CF degradation was observed in the experimental controls (without adding PS, Fe(0) or at neutral pH in the case of the hydrolysis reaction) for any of the three studied reactions. Measured concentrations in all the samples from the control experiments were always higher than 80% of the initial CF concentration (Figure 1). Accordingly, no significant changes in $\delta^{13}\text{C}$ and $\delta^{37}\text{Cl}$ isotope values were detected in the control experiments. In the rest of the experiments, a normal isotope effect was observed for both carbon and chlorine. The isotope results of combined experimental replicates, which were highly consistent for each experimental system, were used to derive C and Cl isotope fractionation values by the use of Rayleigh plots (Figure 2 and SI Figure S3). Further details on kinetics data evaluation, comparison with previous studies and product yields are provided in the SI.

PS Oxidation. The initial carbon and chlorine isotope composition remained constant ($-42 \pm 1\%$ and $-3.1 \pm 0.2\%$, respectively, both $n = 4$) in the control experiments (SI Figure S3A, B). Around 90% of CF removal was observed after 6 days in the PS experiments with an initial PS/CF molar ratio of 40/1 (Figure 1A). In contrast, only 30% and 20% of CF degradation were accomplished after 7 days with initial molar ratios of 10/1 and 5/1, respectively (SI Figure S1). Therefore, isotope ratios were determined only in those samples from the experiments with an initial PS to CF molar ratio of 40/1. Carbon isotope fractionation during oxidation with PS has been shown to be independent of the PS/contaminant molar ratio for chlorinated ethenes and 1,1,1-trichloroethane.^{68,69} Carbon isotope composition exhibited an enrichment of $^{13}\text{C}/^{12}\text{C}$ up to $\delta^{13}\text{C}$ values of $-23.8 \pm 0.5\%$, which resulted in an ϵ_{C} value of $-8 \pm 1\%$ (Figure 2A). Compared to carbon, a much smaller shift in $^{37}\text{Cl}/^{35}\text{Cl}$ was observed (Figure 1A), resulting in $\delta^{37}\text{Cl}$ values up to $-1.9 \pm 0.4\%$ (SI Figure S3AB). An ϵ_{Cl} of $-0.44 \pm 0.06\%$ was obtained (Figure 2B). Neither carbon nor chlorine isotope fractionation associated with this reaction have been reported so far. The pH was kept at circumneutral values (7.0 ± 0.2) during the course of the experiment. This reaction followed pseudo-first-order kinetics with a k' of $0.40 \pm 0.06 \text{ d}^{-1}$ ($R^2 = 0.96$, SI Figure S1). Neither PS consumption nor sulfate production were monitored along the experiments. Chloride concentrations released into solution were measured at the end of the experiment and accounted for between 95% and 110% of the total theoretical CF dechlorination yield, which was calculated assuming release of all the three chlorine atoms. Neither products nor intermediates were detected by headspace GC/MS analysis during the course of the experiments.

Alkaline Hydrolysis. Carbon and chlorine isotope values remained constant ($-41.8 \pm 0.5\%$ and $-2.6 \pm 0.4\%$, respectively, both $n = 5$) in control vials at neutral pH. Under alkaline conditions (the pH remained constant 11.84 ± 0.03 over the duration of the experiment), a 85% decrease in CF concentration within approximately 35 days was observed (Figure 1B). Alkaline hydrolysis induced a significant isotope effect, resulting in $\delta^{13}\text{C}$ and $\delta^{37}\text{Cl}$ values up to $+70.6 \pm 0.3\%$ and $+5.7 \pm 0.4\%$, respectively, after 85% CF removal (SI Figure S3C, D). An ϵ_{C} of $-57 \pm 5\%$ (Figure 2C) and ϵ_{Cl} of $-4.4 \pm 0.4\%$ (Figure 2D) were determined. So far, the only reported carbon isotope fractionation value for CF alkaline hydrolysis was $-53 \pm 3\%$ at a pH range from 11.9 to 12.7,²⁴ which is comparable, within uncertainty, to that obtained in the present study. Carbon isotope fractionation is therefore independent of the pH in the tested range (from 11.8 to 12.7). To our knowledge chlorine isotope fractionation for this reaction has not been reported up to now. The reaction followed pseudo-first-order kinetics ($R^2 = 0.92$, SI Figure S1) with a k' of $0.052 \pm 0.008 \text{ d}^{-1}$, which is in agreement with a previously reported rate constant of $0.047 \pm 0.004 \text{ d}^{-1}$ obtained at a similar pH 11.9 ± 0.1 .²⁴ No particular attempts were made to identify potential products of CF degradation, such as carbon monoxide (CO), formate (HCO_2^-), and chloride (Cl^-). In our previous work, excellent chlorine balances were achieved in similar experiments, indicating that CF was completely dehalogenated without accumulation of chlorinated intermediates.²⁴

Fe(0) Dechlorination. CF in the controls without Fe(0) at pH 6.3 ± 0.2 did not show any changes in carbon and chlorine isotope composition ($\delta^{13}\text{C} = -47.8 \pm 0.5\%$, $n = 4$ and $\delta^{37}\text{Cl} = -3.2 \pm 0.2\%$, $n = 6$, respectively). In the presence of mill-sized Fe(0), CF isotope signatures of both elements showed significant changes leading up to values of $\delta^{13}\text{C} = +35.9 \pm 0.5\%$ and $\delta^{37}\text{Cl} = +1.7 \pm 0.1\%$, respectively, after 84% CF removal (SI Figure S3E, F). Isotope fractionation values of $\epsilon_{\text{C}} = -33 \pm 11\%$ and $\epsilon_{\text{Cl}} = -3 \pm 1\%$ were determined (Figure 2E and F). The obtained ϵ_{C} was not significantly different from ϵ_{C} of $-29 \pm 2\%$ reported recently after 50% of CF dechlorination by commercial microsized Fe(0).²⁹ Chlorine isotope fractionation associated with this reaction has not been reported yet. The pH did not vary significantly over the duration of the experiment (6.2 ± 0.2). The degradation kinetics followed a pseudo-first-order rate law at the beginning of the reaction but after 30 h the disappearance of CF almost stopped (Figure 1C). For Fe(0)-mediated dechlorination of chlorinated ethenes, iron surface passivation due to reactive site saturation by iron hydroxide precipitates has been suggested as the cause of increased reaction half-lives and deviations from pseudo-first-order kinetics at later stages of a reaction.⁷⁰ The obtained k' was $0.07 \pm 0.01 \text{ h}^{-1}$ ($R^2 = 0.93$, SI Figure S1), which corresponds to a k_{SA} of $2.1 \pm 0.4 \times 10^{-2} \text{ L m}^{-2} \text{ d}^{-1}$ (see SI).

DCM and free chloride were detected as final products in Fe(0) experiments, whereas no compounds different from CF appeared in the control experiments without iron. The yield of DCM, defined as the moles of product formed per mole of CF transformed ($\text{DCM}_t/(\text{CF}_0 - \text{CF}_t)$), where subscripts 0 and t indicate initial time and different sampling times, respectively) ranged from 0 to 2.4% over time, showing that accumulation of DCM only accounted for a small fraction of the initial CF. DCM was depleted in ^{13}C compared to the initial isotopic composition of the substrate (CF). DCM showed a trend toward higher $\delta^{13}\text{C}$ values, reflecting the enrichment trend of

Table 1. Carbon and Chlorine Isotope Fractionation (ϵ_C and ϵ_{Cl} , Respectively), Apparent Kinetic Isotope Effects (AKIE_C and AKIE_{Cl}, Respectively) and Dual Isotope Slopes ($\Lambda = \Delta\delta^{13}C/\Delta\delta^{37}Cl$) Values Obtained for the Three Studied CF Transformation Pathways: Oxidation with Thermally-Activated PS, Alkaline Hydrolysis and Fe(0)-Based Reductive Dechlorination^a

experiment	reaction mechanism	ϵ_{bulkC} (‰)	R^2	AKIE _C	ϵ_{bulkCl} (‰)	R^2	AKIE _{Cl}	Λ
persulfate	oxidative C–H bond cleavage	-8 ± 1	0.94	1.008 ± 0.001	-0.44 ± 0.06	0.97	1.00045 ± 0.00004^b	17 ± 2
alkaline hydrolysis	E1 _{CB} elimination	-57 ± 5	0.97	1.061 ± 0.006	-4.4 ± 0.4	0.96	1.0133 ± 0.0004	13.0 ± 0.8
Fe(0)	reductive dechlorination by C–Cl bond cleavage	-33 ± 11	0.82	1.034 ± 0.012	-3 ± 1	0.85	1.008 ± 0.001	8 ± 2

^aThe uncertainty of ϵ , AKIE and Λ values corresponds to the 95% CI. In all cases, AKIE_C was calculated using $x = z = 1$ in eq S16. For both alkaline hydrolysis and dechlorination by Fe(0), AKIE_{Cl} was calculated using $x = z = 3$ as all C–Cl bonds are equivalent and compete for reaction. For oxidation with PS, as there is not primary chlorine isotopic effect, the secondary AKIE_{Cl} was also calculated by eq S16 using in this case $x = 3$ and $z = 1$ because no specific bond containing Cl is broken, and there is, therefore, no intramolecular competition for this bond. ^bsecondary isotope effect.

the CF from which it was formed (SI Figure S3E). The DCM-related isotope fractionation $\epsilon_{substrate \rightarrow product}^C$ was estimated as $-19 \pm 3\%$ using the fitting parameter, $D(\delta^{13}C) = +13 \pm 2\%$ ($R^2 = 0.62$) (see equations in the SI). This discrepancy between the product-related and the substrate-related isotope fractionations ($\epsilon_{CF \rightarrow DCM}^C = -19 \pm 3\%$ vs $\epsilon_C = -33 \pm 11\%$) is likely attributable to the formation of other products including isotope-sensitive branching from the parent compound or intermediates, such as a dichloromethyl radical (SI Figure S4), to DCM.⁷¹ However, due to the lack of DCM isotope signatures at early stages of reaction, such interpretations must be conducted with caution.

3.2. Mechanistic Considerations. For further elucidation of the reaction mechanism, AKIE values were calculated using eq S16, to characterize the isotope effect of the cleavage of the chemical bond at the reactive positions. Table 1 summarizes the obtained results and proposed reaction pathways for the three studied reactions are shown in Figure 3 and discussed in detail in the SI.

The AKIE_C for the oxidation reaction was 1.008 ± 0.001 , which is within the range of reported carbon AKIEs for oxidative C–H bond cleavage for both abiotic (1.008–1.015) and microbial oxidation reactions (1.001–1.044) (SI Table S2), indicating that the observed fractionation was dominated by the KIE associated with oxidative cleavage of a C–H bond. A similar AKIE_C value (1.008) was obtained for 1,1,1-TCA oxidation by thermally activated PS⁶⁵ from which it was suggested that the first reaction step was the rupture of the C–H bond and the abstraction of the hydrogen atom from the molecule by the attack of any of the radicals formed after persulfate activation.^{65,72,73} The secondary AKIE_{Cl} estimated in the present experiments (1.00045 ± 0.00004) also points to an oxidative reaction, where there is not initial C–Cl bond cleavage and thus a primary chlorine kinetic isotope effect is not expected. A reaction pathway involving the cleavage of the C–H as the rate-limiting step is proposed (Figure 3A and SI). In order to track more confidently the proposed mechanism, hydrogen isotope fractionation during CF oxidation with thermally activated PS might be further measured.

During alkaline hydrolysis, CF is abiotically dechlorinated to carbon monoxide and formate.^{74,75} A stepwise elimination mechanism (E1_{CB}) has been proposed for this reaction.^{24,74,76,77} This mechanism consists of the rapid, reversible, base-catalyzed deprotonation of the molecule with the formation of a trichloromethyl carbanion (:CCl₃⁻), followed by the rate-determining unimolecular loss of a chloride ion to produce the reactive intermediate dichlorocarbene (CCl₂), which is then rapidly transformed into carbon monoxide and formate (SI Figure S4). If this is the case, as the deprotonation

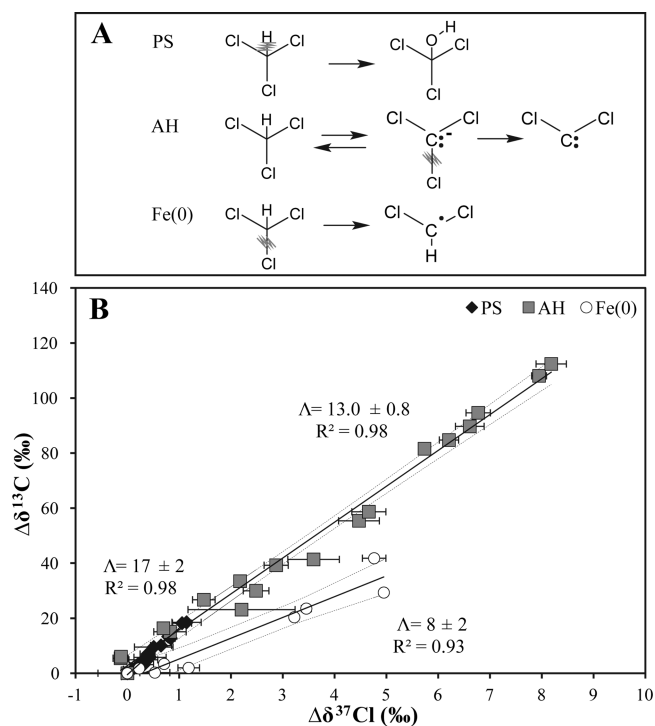


Figure 3. (A) Proposed reaction pathways for CF degradation by the three studied reactions. More details are given in the SI. (B) Dual C–Cl isotope plot for CF degradation by the three studied pathways: oxidation by thermally activated PS (PS), alkaline hydrolysis (AH) and dechlorination by Fe(0) (Fe(0)). Data from duplicate experiments were combined. Lines are linear regressions of the data sets with 95% CI (dashed lines). Error bars show uncertainty in isotope measurements. Note that error bars of $\delta^{13}C$ values are smaller than the symbols.

step is reversible and the loss of a chloride ion is the rate-determining step, both carbon and chlorine primary isotope effects in the CF molecule are expected during this process. In the present experiments, an AKIE_C of 1.061 ± 0.006 was obtained for alkaline hydrolysis, which is consistent with the Streitwieser limit for a primary carbon KIE in C–Cl bonds (1.057, SI Table S2)^{37,78} and is equivalent, within the given 95% CI, to the value previously found by Torrentó et al.²⁴ (1.056 ± 0.003). The AKIE_{Cl} was calculated as 1.0133 ± 0.0004 , which is equal to the maximum expected KIE_{Cl} for cleavage of a C–Cl bond (1.013, SI Table S2),³⁷ indicating the involvement of a C–Cl bond. In principle, the Cl kinetic isotope effect estimated in the present study is, therefore, consistent with the occurrence of a carbanion mechanism

(Figure 3A) but also with a C–Cl bond cleavage via a concerted one-step S_N2 nucleophilic substitution mechanism. Nevertheless, based on energy considerations, the E_{1CB} mechanism seems more plausible for this reaction (see the SI for further discussion). Further deuterium-exchange experiments might be performed to confirm the existence of a carbanion intermediate as a way to further corroborate the occurrence of the stepwise elimination mechanism.⁷⁹

In the case of reductive dechlorination by Fe(0), an $AKIE_C$ of 1.034 ± 0.012 was obtained, which is similar to the value of 1.030 ± 0.007 obtained by Lee et al.²⁹ and within the $AKIE_C$ range for the reductive cleavage of C–Cl bonds reported in the literature (1.003–1.060) (SI Table S2). In fact, most $AKIE_C$ values for reductive dehalogenation fall in the range of 1.027 and 1.033, which corresponds to about 50% bond cleavage when considering a Streitwieser limit for a C–Cl bond of 1.057 for complete bond cleavage in an infinitely late transition state.⁸⁰ Regarding $AKIE_{Cl}$, a value of 1.008 ± 0.001 was calculated, which is also about 50% of the Streitwieser limit for KIE_{Cl} in C–Cl bonds (1.013).³⁷ Similar $AKIE_{Cl}$ values, ranging from 1.008 to 1.016 for abiotic reductive dechlorination and from 1.004 to 1.011 for biotic reductive dechlorination, have been previously reported for chlorinated methanes, ethenes and ethanes (SI Table S2). Therefore, both C and Cl- $AKIEs$ pointed to cleavage of a C–Cl bond in the first rate-limiting step, which is compatible with the two-step pathway that is commonly hypothesized for this reaction (see SI). The first step may, for example, involve the transfer of a single electron from the metal surface causing the removal of a chlorine atom and the formation of a dichloromethyl radical ($\cdot CHCl_2$) (Figure 3A).

3.3. Dual Element Isotope Plot. Figure 3B shows the dual C–Cl isotope plot for the reactions of this study. A linear correlation between $\Delta\delta^{13}C$ and $\Delta\delta^{37}Cl$ was observed for the three studied transformation mechanisms ($r^2 \geq 0.92$). A comparison of the slopes ($\Lambda = \Delta\delta^{13}C / \Delta\delta^{37}Cl$) for the regression lines was performed by analysis of covariance (ANCOVA). Statistical significance was accepted at the $p < 0.05$ level. There is no significant statistical difference between oxidation by thermally activated persulfate (17 ± 2) and alkaline hydrolysis (13.0 ± 0.8) slopes (ANCOVA, $p = 0.2$). In contrast, these results differ significantly (ANCOVA, $p < 0.0001$) from the slope observed during CF reductive dechlorination by Fe(0) (8 ± 2).

Hence, although different mechanisms are involved in CF degradation by oxidation by thermally activated PS (cleavage of a C–H bond) and by alkaline hydrolysis (cleavage of a C–Cl bond), the obtained Λ values for both degradation reactions are not significantly different. This may be explained by considerations for carbon and chlorine isotope effects. *Carbon.* As expected, the obtained $AKIE_C$ value for CF degradation by oxidation with heat-activated PS is smaller than for alkaline hydrolysis. The higher the mass of the bonding partner, the greater is typically the primary kinetic isotope effects.³⁷ Hence it can be explained that carbon isotope fractionation associated with C–Cl bond cleavage is greater than in C–H bond cleavage since the carbon atom is bound to a heavier atom (chlorine vs hydrogen). *Chlorine.* This difference, however, is matched by similar differences in chlorine isotope fractionation. On the one hand, C–Cl bond cleavage involves a primary $AKIE_{Cl}$, which is clearly greater than a secondary $AKIE_{Cl}$ next to a reacting C–H bond. On the other hand, this primary $AKIE_{Cl}$ is “diluted” in ϵ_{Cl} due to the intramolecular competition

between three chemically equivalent C–Cl bonds ($z = 3$ in eq S16), whereas the simultaneous secondary $AKIE_{Cl}$ of three Cl atoms are not diluted ($z = 1$). By coincidence, the interplay of these factors results in a similar reduction of carbon as of chlorine isotope fractionation so that similar Λ are obtained. This unexpected result restrains the use of C–Cl isotope plots for distinguishing these reactions in the field and highlights the need to apply this approach with precaution and using complementary tools for identification of degradation mechanisms in the field (e.g., complementary hydrogen isotope analysis).

4. ENVIRONMENTAL SIGNIFICANCE

Carbon and chlorine isotope fractionation of CF during oxidation with heat-activated PS, by alkaline hydrolysis and by reductive dechlorination with Fe(0) was studied in batch experiments in order to explore the potential of CSIA for the identification of reaction mechanisms in the monitoring of remediation strategies at contaminated sites. For the first time, carbon isotope fractionation values (for heat-activated PS) and chlorine isotope fractionation values (for the three reactions) were determined. These new ϵ values increase the options of using CSIA for estimating the extent of contaminant degradation at field sites where remediation strategies are implemented that rely on induced abiotic transformations of CF. Based on the obtained ϵ values, it is likely that changes in isotope values in the field may be larger than 2‰ for carbon and 0.4‰ (for GC/IRMS instruments) or 2‰ (for GC/qMS instruments) for chlorine - these are the significant levels that have been suggested as reliable indicators of degradation.^{34,81} Even with the relatively small carbon fractionation obtained for CF oxidation by PS ($-8 \pm 1‰$) and chlorine isotope fractionation observed for Fe(0)-mediated reductive dechlorination ($-3 \pm 1‰$), shifts in CF isotopic composition will be already detectable with a reasonable accuracy if the substrate is degraded by 20% and 25–50%, respectively.

Although only the reductive dechlorination showed significantly statistically different C–Cl isotope slope compared with the other two reactions (oxidation and alkaline hydrolysis), the dual isotope approach might still be used to identify different CF degradation mechanisms in the field, which would (or not necessarily) take place at the same time. For example, the coupling of two common treatments—ISCO and in situ bioremediation—has been shown not only to be feasible, but in many cases also to be able to provide a more efficient and extensive cleanup of contaminated sites.⁸² In the case of PS, the anaerobic environment that is created following the consumption of the oxidant is ideal for CF microbial dehalogenation under sulfate reduction conditions to be enhanced. Enhanced CF bioremediation has also been observed when combining Fe(0) and methanogens that use the cathodic hydrogen generated by iron corrosion for cometabolic degradation of CF^{83–85} or even better by dehalorespiring bacteria which are not inhibited at certain concentrations of CF.²⁹ Therefore, there would be an increasing number of case studies, where CF degradation due to PS application or Fe(0) barriers should be distinguished from biotic reductive dechlorination in the field. Although chlorine isotope fractionation during biotic CF dechlorination remains to be evaluated in detail, as well as the effect in CF degradation of Fe(0) aging or the presence of Fe(0) impurities such as graphite,⁸⁶ the dual C–Cl slopes obtained in the present work sets the grounds for the potential application of this approach

for assessing if CF abiotic reductive dechlorination performed by Fe(0)-PRB or naturally occurring iron-bearing minerals would be or not distinguishable from microbial reductive dechlorination.

Although CF anaerobic biodegradation has been reported to occur mainly via cometabolic dechlorination or by dehalorespiration,⁸ an alternative pathway was suggested in the presence of cobalamins and involving CF hydrolysis.^{87,88} The mechanism of this reaction is not well-known, but it presumably involves the cobalamin-catalyzed conversion of CF to a monochloro-carbene, which would be subsequently hydrolyzed to formaldehyde. The produced formaldehyde could then be oxidized to CO or formate and finally to CO₂. The abiotic alkaline hydrolysis reaction characterized in the present study might be used as a reference system for this suggested CF biotic hydrolysis in future dual isotope-CSIA studies.

Finally, due to the significant difference between the C–Cl isotope slope of CF oxidation and reductive dechlorination, the dual isotope approach might be in addition useful for distinguishing between aerobic and anaerobic CF biodegradation pathways. CF aerobic biodegradation only occurs during oxidative cometabolism with other primary substrates such as methane, butane or toluene by oxygenase-expressing microorganisms.⁸ The pathway of CF cooxidation starts by insertion of one oxygen atom into the molecule via H abstraction with phosgene as intermediate and final mineralization to chloride and CO₂. The chemical mechanism of CF oxidation is variable among the various existent monooxygenases, but the rate-limiting step is expected to be the cleavage of the C–H bond.

In conclusion, our study established an expedient base with carbon and chlorine isotope fractionation during three abiotic CF transformation mechanisms. Further research is needed in order to explore if other CF natural degradation pathways (for example naturally occurring iron-bearing minerals as well as aerobic and anaerobic degraders) might be similar to or different from the patterns generated in this study. Such information will allow connecting dual-plot slopes to known reaction mechanisms with the aim to distinguish different degradation processes in the field. This distinction would be important for better monitoring the success of remediation strategies at contaminated sites.

■ ASSOCIATED CONTENT

Supporting Information

The Supporting Information is available free of charge on the ACS Publications website at DOI: 10.1021/acs.est.7b00679.

Chemicals; analytical methods; further discussion in kinetics; calculation of AKIE values; calculation of isotope trend for DCM in the Fe(0) experiment; carbon and chlorine isotope fractionation patterns; further discussion in reaction pathways; comparison of ϵ and AKIE values for C and Cl isotopes in different studies (PDF)

■ AUTHOR INFORMATION

Corresponding Author

*Phone: +41 32 718 26 49; fax: +41 32 718 26 03; e-mail: clara.torrento@unine.ch.

ORCID

Clara Torrentó: 0000-0003-1480-2744

Jordi Palau: 0000-0001-9492-7306

Diana Rodríguez-Fernández: 0000-0002-2515-9945

Mònica Rosell: 0000-0003-1563-8595

Martin Elsner: 0000-0003-4746-9052

Notes

The authors declare no competing financial interest.

■ ACKNOWLEDGMENTS

This study was financed through the following projects: CGL2011-29975-C04-01 and CGL2014-57215-C4-1-R from the Spanish Government, 2014SGR1456 from the Catalan Government and a Marie Curie Career Integration Grant in the framework of the IMOTEC-BOX project (PCIG9-GA-2011-293808) within the European Union seventh Framework Programme. The experiments and analysis performed in Helmholtz Zentrum München by D. Rodríguez-Fernández were supported by the FPU2012/01615 contract. We want to thank the Scientific and Technological Centers of the University of Barcelona (CCiTUB) for their services. We thank the editor and three anonymous reviewers for comments that improved the quality of the manuscript.

■ REFERENCES

- (1) Laturmus, F.; Haselmann, K. F.; Borch, T.; Gron, C. Terrestrial natural sources of trichloromethane (chloroform, CHCl₃) - An overview. *Biogeochemistry* **2002**, *60*, 121–139.
- (2) Albers, C. N.; Jacobsen, O. S.; Flores, E. M. M.; Pereira, J. S. F.; Laier, T. Spatial variation in natural formation of chloroform in the soils of four coniferous forests. *Biogeochemistry* **2011**, *103*, 317–334.
- (3) Hunkeler, D.; Laier, T.; Breider, F.; Jacobsen, O. S. Demonstrating a natural origin of chloroform in groundwater using stable carbon isotopes. *Environ. Sci. Technol.* **2012**, *46*, 6096–6101.
- (4) Rossberg, M.; Lendle, W.; Pfeleiderer, G.; Tögel, A.; Torkelson, T. R.; Beutel, K. K. *Chloromethanes. Ullmann's Encyclopedia of Industrial Chemistry*, 2011.
- (5) Zogorski, J. S.; Carter, J. M.; Ivahnenko, T.; Lapham, W. W.; Moran, M. J.; Rowe, B. L.; Squillace, P. J.; Toccalino, P. L. *The Quality of Our Nation's Waters - Volatile Organic Compounds in the Nation's Ground Water and Drinking-Water Supply Wells*; U.S. Geological Survey Circular 1292, 2006.
- (6) Dobrzyńska, E.; Pośniak, M.; Szewczyńska, M.; Buszewski, B. Chlorinated volatile organic compounds: Old, however, actual analytical and toxicological problem. *Crit. Rev. Anal. Chem.* **2010**, *40*, 41–57.
- (7) Agency for toxic substances and disease registry (ATSDR). Priority List of Hazardous Substances 2015, <http://www.atsdr.cdc.gov/spl/index.html>.
- (8) Cappelletti, M.; Frascari, D.; Zannoni, D.; Fediet, S. Microbial degradation of chloroform. *Appl. Microbiol. Biotechnol.* **2012**, *96*, 1395–1409.
- (9) Grostern, A.; Duhamel, M.; Dworzczek, S.; Edwards, E. A. Chloroform respiration to dichloromethane by a *Dehalobacter* population. *Environ. Microbiol.* **2010**, *12*, 1053–1060.
- (10) Lee, M.; Low, A.; Zemb, O.; Koenig, J.; Michaelsen, A.; Manefield, M. Complete chloroform dechlorination by organochlorine respiration and fermentation. *Environ. Microbiol.* **2012**, *14*, 883–894.
- (11) Chan, C. C. H.; Mundle, S. O. C.; Eckert, T.; Liang, X.; Tang, S.; Lacrampe-Couloume, G.; Edwards, E. A.; Sherwood-Lollar, B. Large carbon isotope fractionation during biodegradation of chloroform by *Dehalobacter* cultures. *Environ. Sci. Technol.* **2012**, *46*, 10154–10160.
- (12) Tang, S.; Edwards, E. A. Identification of *Dehalobacter* reductive dehalogenases that catalyze dechlorination of chloroform, 1,1,1-trichloroethane and 1,1-dichloroethane. *Philos. Trans. R. Soc., B* **2013**, *368*, 20120318.
- (13) Deshpande, N. P.; Wong, Y. K.; Manefield, M.; Wilkins, M. R.; Lee, M. Genome sequence of *Dehalobacter* UNSWDHB, a chloroform dechlorinating bacterium. *Genome Announc.* **2013**, *1*, e00720–13.

- (14) Ding, C.; Zhao, S.; He, J. A *Desulfitobacterium* sp. strain PR reductively dechlorinates both 1,1,1-trichloroethane and chloroform. *Environ. Microbiol.* **2014**, *16*, 3387–3397.
- (15) Justicia-Leon, S. D.; Higgins, S.; Mack, E. E.; Griffiths, D. R.; Tang, S.; Edwards, E. A.; Löffler, F. E. Bioaugmentation with distinct *Dehalobacter* strains achieves chloroform detoxification in microcosms. *Environ. Sci. Technol.* **2014**, *48*, 1851–1858.
- (16) Duhamel, M.; Wehr, S. D.; Yu, L.; Rizvi, H.; Seepersad, D.; Dworatzek, S.; Cox, E. E.; Edwards, E. A. Comparison of anaerobic dechlorinating enrichment cultures maintained on tetrachloroethene, trichloroethene, cis-dichloroethene and vinyl chloride. *Water Res.* **2002**, *36*, 4193–4202.
- (17) Maymó-Gatell, X.; Nijenhuis, I.; Zinder, S. H. Reductive dechlorination of cis-1,2-dichloroethene and vinyl chloride by *Dehalococcoides ethenogenes*. *Environ. Sci. Technol.* **2001**, *35*, 516–521.
- (18) Kenneke, J. F.; Weber, E. J. Reductive dehalogenation of halomethanes in iron- and sulfate-reducing sediments. 1. Reactivity pattern analysis. *Environ. Sci. Technol.* **2003**, *37*, 713–720.
- (19) Huling, S. G.; Pivetz, B. E. *In Situ Chemical Oxidation-Engineering Issue*, EPA/600/R-06/072; U.S. Environmental Protection Agency Office of Research and Development, National Risk Management Research Laboratory: Cincinnati, OH, 2006.
- (20) Huang, K. C.; Zhao, Z.; Hoag, G. E.; Dahmani, A.; Block, P. A. Degradation of volatile organic compounds with thermally activated persulfate oxidation. *Chemosphere* **2005**, *61*, 551–560.
- (21) Waldemer, R. H.; Tratnyek, P. G.; Johnson, R. L.; Nurmi, J. T. Oxidation of chlorinated ethenes by heat-activated persulfate: Kinetics and products. *Environ. Sci. Technol.* **2007**, *41*, 1010–1015.
- (22) Tsitonaki, A.; Petri, B.; Crimi, M.; Mosbaek, H.; Siegrist, R. L.; Bjerg, P. L. In situ chemical oxidation of contaminated soil and groundwater using persulfate: a review. *Crit. Rev. Environ. Sci. Technol.* **2010**, *40*, 55–91.
- (23) Zhu, X.; Du, E.; Ding, H.; Lin, Y.; Long, T.; Li, H.; Wang, L. QSAR modeling of VOCs degradation by ferrous-activated persulfate oxidation. *Desalin. Water Treat.* **2016**, *57*, 1–15.
- (24) Torrentó, C.; Audí-Miró, C.; Bordeleau, G.; Marchesi, M.; Rosell, M.; Otero, N.; Soler, A. The use of alkaline hydrolysis as a novel strategy for chloroform remediation: feasibility of using urban construction wastes and evaluation of carbon isotopic fractionation. *Environ. Sci. Technol.* **2014**, *48*, 1869–1877.
- (25) Gillham, R. W.; O'Hannesin, S. F. Enhanced reduction of halogenated aliphatics by zero-valent iron. *Groundwater* **1994**, *32*, 958–967.
- (26) Matheson, L. J.; Tratnyek, P. G. Reductive dehalogenation of chlorinated methanes by iron metal. *Environ. Sci. Technol.* **1994**, *28*, 2045–2053.
- (27) Johnson, T. L.; Scherer, M. M.; Tratnyek, P. G. Kinetics of halogenated organic compound reduction by iron metal. *Environ. Sci. Technol.* **1996**, *30*, 2634–2640.
- (28) Feng, J.; Lim, T.-T. Pathways and kinetics of carbon tetrachloride and chloroform reductions by nano-scale Fe and Fe/Ni particles: comparison with commercial micro-scale Fe and Zn. *Chemosphere* **2005**, *59*, 1267–1277.
- (29) Lee, M.; Wells, E.; Wong, Y. K.; Koenig, J.; Adrian, L.; Richnow, H. H.; Manefield, M. Relative contributions of *Dehalobacter* and zerovalent iron in the degradation of chlorinated methanes. *Environ. Sci. Technol.* **2015**, *49*, 4481–4489.
- (30) O'Hannesin, S. F.; Gillham, R. W. Long-term performance of an in situ "iron wall" for remediation of VOCs. *Groundwater* **1998**, *36*, 164–170.
- (31) Wilkin, R. T.; Acree, S. D.; Ross, R. R.; Puls, R. W.; Lee, T. R.; Woods, L. L. Fifteen-year assessment of a permeable reactive barrier for treatment of chromate and trichloroethylene in groundwater. *Sci. Total Environ.* **2014**, *468–469*, 186–194.
- (32) Zhang, W.-X. Nanoscale iron particles for environmental remediation: An overview. *J. Nanopart. Res.* **2003**, *5*, 323–332.
- (33) Elsner, M.; Lacrampe-Couloume, G.; Mancini, S. A.; Burns, L.; Sherwood Lollar, B. Carbon isotope analysis to evaluate nanoscale Fe(0) treatment at a chlorohydrocarbon contaminated site. *Groundwater Monit. Rem.* **2010**, *30*, 79–95.
- (34) Meckenstock, R. U.; Barbara Morasch, B.; Griebler, C.; Richnow, H. H. Stable isotope fractionation analysis as a tool to monitor biodegradation in contaminated aquifers. *J. Contam. Hydrol.* **2004**, *75*, 215–255.
- (35) Elsner, M. Stable isotope fractionation to investigate natural transformation mechanisms of organic contaminants: principles, prospects and limitations. *J. Environ. Monit.* **2010**, *12*, 2005–2031.
- (36) Mariotti, A.; Germon, J. C.; Hubert, P.; Kaiser, P.; Letolle, R.; Tardieux, A.; Tardieux, P. Experimental determination of nitrogen kinetic isotope fractionation: Some principles; illustration for the denitrification and nitrification processes. *Plant Soil* **1981**, *62*, 413–430.
- (37) Elsner, M.; Zwank, L.; Hunkeler, D.; Schwarzenbach, R. P. A new concept linking observable stable isotope fractionation to transformation pathways of organic pollutants. *Environ. Sci. Technol.* **2005**, *39*, 6896–6916.
- (38) Hofstetter, T. B.; Berg, M. Assessing transformation processes of organic contaminants by compound-specific stable isotope analyses. *TrAC, Trends Anal. Chem.* **2011**, *30*, 618–627.
- (39) Mancini, S. A.; Hirschorn, S. K.; Elsner, M.; Lacrampe-Couloume, G.; Sleep, B. E.; Edwards, E. A.; Sherwood Lollar, B. Effects of trace element concentration on enzyme controlled stable isotope fractionation during aerobic biodegradation of toluene. *Environ. Sci. Technol.* **2006**, *40*, 7675–7681.
- (40) Penning, H.; Cramer, C. J.; Elsner, M. Rate-dependent carbon and nitrogen kinetic isotope fractionation in hydrolysis of isoproturon. *Environ. Sci. Technol.* **2008**, *42*, 7764–7771.
- (41) Renpenning, J.; Keller, S.; Cretnik, S.; Shouakar-Stash, O.; Elsner, M.; Schubert, T.; Nijenhuis, I. Combined C and Cl isotope effects indicate differences between corrinoids and enzyme (*Sulfur-oxidizing multivivans* PceA) in reductive dehalogenation of tetrachloroethene, but not trichloroethene. *Environ. Sci. Technol.* **2014**, *48*, 11837–11845.
- (42) Renpenning, J.; Rapp, L.; Nijenhuis, I. Substrate hydrophobicity and cell composition influence the extent of rate limitation and masking of isotope fractionation during microbial reductive dehalogenation of chlorinated ethenes. *Environ. Sci. Technol.* **2015**, *49*, 4293–4301.
- (43) Tobler, N. B.; Hofstetter, T. B.; Schwarzenbach, R. P. Carbon and hydrogen isotope fractionation during anaerobic toluene oxidation by *Geobacter metallireducens* with different Fe(III) phases as terminal electron acceptors. *Environ. Sci. Technol.* **2008**, *42*, 7786–7792.
- (44) Vogt, C.; Cyrus, E.; Herklotz, I.; Schlosser, D.; Bahr, A.; Herrmann, S.; Richnow, H. H.; Fischer, A. Evaluation of toluene degradation pathways by two-dimensional stable isotope fractionation. *Environ. Sci. Technol.* **2008**, *42*, 7793–7800.
- (45) Abe, Y.; Aravena, R.; Zopfi, J.; Shouakar-Stash, O.; Cox, E.; Roberts, J. D.; Hunkeler, D. Carbon and chlorine isotope fractionation during aerobic oxidation and reductive dechlorination of vinyl chloride and cis-1,2-dichloroethene. *Environ. Sci. Technol.* **2009**, *43*, 101–107.
- (46) Audí-Miró, C.; Cretnik, S.; Otero, N.; Palau, J.; Shouakar-Stash, O.; Soler, A.; Elsner, M. Cl and C isotope analysis to assess the effectiveness of chlorinated ethene degradation by zero-valent iron: Evidence from dual element and product isotope values. *Appl. Geochem.* **2013**, *32*, 175–183.
- (47) Cretnik, S.; Thoreson, K. A.; Bernstein, A.; Ebert, K.; Buchner, D.; Laskov, C.; Haderlein, S.; Shouakar-Stash, O.; Kliegman, S.; McNeill, K.; Elsner, M. Reductive dechlorination of TCE by chemical model systems in comparison to dehalogenating bacteria: Insights from dual element isotope analysis ($^{13}\text{C}/^{12}\text{C}$, $^{37}\text{Cl}/^{35}\text{Cl}$). *Environ. Sci. Technol.* **2013**, *47*, 6855–6863.
- (48) Kuder, T.; van Breukelen, B. M.; Vanderford, M.; Philp, P. 3D-CSIA: Carbon, chlorine, and hydrogen isotope fractionation in transformation of TCE to ethene by a *Dehalococcoides* culture. *Environ. Sci. Technol.* **2013**, *47*, 9668–9677.
- (49) Badin, A.; Buttet, G.; Maillard, J.; Holliger, C.; Hunkeler, D. Multiple dual C–Cl isotope patterns associated with reductive

dechlorination of tetrachloroethene. *Environ. Sci. Technol.* **2014**, *48*, 9179–9186.

(50) Palau, J.; Cretnik, S.; Shouakar-Stash, O.; Höche, M.; Elsner, M.; Hunkeler, M. C and Cl isotope fractionation of 1,2-dichloroethane displays unique $\delta^{13}\text{C}/\delta^{37}\text{Cl}$ patterns for pathway identification and reveals surprising C–Cl bond involvement in microbial oxidation. *Environ. Sci. Technol.* **2014**, *48*, 9430–9437.

(51) Poulson, S. R.; Drever, J. I. Stable isotope (C, Cl, and H) fractionation during vaporization of trichloroethylene. *Environ. Sci. Technol.* **1999**, *33*, 3689–3694.

(52) Slater, G. F.; Ahad, J. M. E.; Sherwood Lollar, B.; Allen-King, R. M.; Sleep, B. E. Carbon isotope effects resulting from equilibrium sorption of dissolved VOCs. *Anal. Chem.* **2000**, *72*, 5669–5672.

(53) Wang, Y.; Huang, Y. S. Hydrogen isotopic fractionation of petroleum hydrocarbons during vaporization: Implications for assessing artificial and natural remediation of petroleum contamination. *Appl. Geochem.* **2003**, *18*, 1641–1651.

(54) Bouchard, D.; Hohener, P.; Hunkeler, D. Carbon isotope fractionation during volatilization of petroleum hydrocarbons and diffusion across a porous medium: a column experiment. *Environ. Sci. Technol.* **2008**, *42*, 7801–7806.

(55) Kuder, T.; Philp, P.; Allen, J. Effects of volatilization on carbon and hydrogen isotope ratios of MTBE. *Environ. Sci. Technol.* **2009**, *43*, 1763–1768.

(56) Jeannotat, S.; Hunkeler, D. Chlorine and carbon isotopes fractionation during volatilization and diffusive transport of trichloroethene in the unsaturated zone. *Environ. Sci. Technol.* **2012**, *46*, 3169–3176.

(57) Wanner, P.; Hunkeler, D. Carbon and chlorine isotopologue fractionation of chlorinated hydrocarbons during diffusion in water and low permeability sediments. *Geochim. Cosmochim. Acta* **2015**, *157*, 198–212.

(58) Hunkeler, D.; Meckenstock, R. U.; Sherwood Lollar, B.; Schmidt, T.; Wilson, J.; Schmidt, T.; Wilson, J. *A Guide for Assessing Biodegradation and Source Identification of Organic Ground Water Contaminants Using Compound Specific Isotope Analysis (CSIA)*, PA 600/R-08/148; US EPA: 2008; www.epa.gov/ada.

(59) Van Breukelen, B. M. Extending the Rayleigh equation to allow competing isotope fractionating pathways to improve quantification of biodegradation. *Environ. Sci. Technol.* **2007**, *41*, 4004–4010.

(60) Hunkeler, D.; Abe, Y.; Broholm, M. M.; Jeannotat, S.; Westergaard, C.; Jacobsen, C. S.; Aravena, R.; Bjerg, P. L. Assessing chlorinated ethene degradation in a large scale contaminant plume by dual carbon-chlorine isotope analysis and quantitative PCR. *J. Contam. Hydrol.* **2011**, *119*, 69–79.

(61) Wiegert, C.; Aeppli, C.; Knowles, T.; Holmstrand, H.; Evershed, R.; Pancost, R. D.; Macháčeková, J.; Gustafsson, O. Dual carbon-chlorine stable isotope investigation of sources and fate of chlorinated ethenes in contaminated groundwater. *Environ. Sci. Technol.* **2012**, *46*, 10918–10925.

(62) Audí-Miró, C.; Cretnik, S.; Torrentó, C.; Rosell, M.; Shouakar-Stash, O.; Otero, N.; Palau, J.; Elsner, M.; Soler, A. C, Cl and H compound-specific isotope analysis to assess natural versus Fe(0) barrier-induced degradation of chlorinated ethenes at a contaminated site. *J. Hazard. Mater.* **2015**, *299*, 747–754.

(63) Badin, A.; Broholm, M. M.; Jacobsen, C. S.; Palau, J.; Dennis, P.; Hunkeler, D. Identification of abiotic and biotic reductive dechlorination in a chlorinated ethene plume after thermal source remediation by means of isotopic and molecular biology tools. *J. Contam. Hydrol.* **2016**, *192*, 1–19.

(64) Palau, J.; Jamin, P.; Badin, A.; Vanhecke, N.; Haerens, B.; Brouyère, S.; Hunkeler, D. Use of carbon-chlorine dual isotope analysis to assess the degradation pathways of 1,1,1-trichloroethane in groundwater. *Water Res.* **2016**, *92*, 235–243.

(65) Palau, J.; Shouakar-Stash, O.; Hunkeler, D. Carbon and chlorine isotope analysis to identify abiotic degradation pathways of 1,1,1-trichloroethane. *Environ. Sci. Technol.* **2014**, *48*, 14400–14408.

(66) Breider, F.; Hunkeler, D. Investigating chloroperoxidase-catalyzed formation of chloroform from humic substances using stable chlorine isotope analysis. *Environ. Sci. Technol.* **2014**, *48*, 1592–1600.

(67) Heckel, B.; Rodríguez-Fernández, D.; Torrentó, D.; Meyer, A.; Palau, J.; Domènech, C.; Rosell, M.; Soler, A.; Hunkeler, D.; Elsner, D. Compound-specific chlorine isotope analysis of tetrachloro-methane and trichloromethane by GC-IRMS vs. GC-qMS: Method development and evaluation of precision and trueness. *Anal. Chem.* **2017**, *89*, 3411–3420.

(68) Marchesi, M.; Aravena, R.; Sra, K. S.; Thomson, N. R.; Otero, N.; Soler, A.; Mancini, S. Carbon isotope fractionation of chlorinated ethenes during oxidation by Fe²⁺ activated persulfate. *Sci. Total Environ.* **2012**, *433*, 319–322.

(69) Marchesi, M.; Thomson, N. R.; Aravena, R.; Sra, K. S.; Otero, N.; Soler, A. Carbon isotope fractionation of 1,1,1-trichloroethane during base-catalyzed persulfate treatment. *J. Hazard. Mater.* **2013**, *260*, 61–66.

(70) Farrell, J.; Kason, M.; Melitas, N.; Li, T. Investigation of the long-term performance of zero-valent iron for reductive dechlorination of trichloroethylene. *Environ. Sci. Technol.* **2000**, *34*, 514–521.

(71) Neumann, A.; Hofstetter, T. B.; Skarpeli-Liati, M.; Schwarzenbach, R. P. Reduction of polychlorinated ethanes and carbon tetrachloride by structural Fe(II) in smectites. *Environ. Sci. Technol.* **2009**, *43*, 4082–4089.

(72) Gu, X. G.; Lu, S. G.; Li, L.; Qiu, Z. F.; Sui, Q.; Lin, K. F.; Luo, Q. S. Oxidation of 1,1,1-trichloroethane stimulated by thermally activated persulfate. *Ind. Eng. Chem. Res.* **2011**, *50*, 11029–11036.

(73) Xu, M. H.; Gu, X. G.; Lu, S. G.; Qiu, Z. F.; Sui, Q. Role of reactive oxygen species for 1,1,1-trichloroethane degradation in a thermally activated persulfate system. *Ind. Eng. Chem. Res.* **2014**, *53*, 1056–1063.

(74) Hine, J. Carbon dichloride as an intermediate in the basic hydrolysis of chloroform. A mechanism for substitution reactions at a saturated carbon atom. *J. Am. Chem. Soc.* **1950**, *72*, 2438–2445.

(75) Fells, I.; Moelwyn-Hughes, E. A. The kinetics of the hydrolysis of the chlorinated methanes. *J. Chem. Soc.* **1959**, 398–409.

(76) Hine, J.; Ehrenson, S. J. The effect of structure on the relative stability of dihalomethylenes. *J. Am. Chem. Soc.* **1958**, *80*, 824–830.

(77) Valiev, M.; Garrett, B. C.; Tsai, M.-K.; Kowalski, K.; Kathmann, S. M.; Schenter, G. K.; Dupuis, M. Hybrid approach for free energy calculations with high-level methods: Application to the S_N2 reaction of CHCl₃ and OH⁻ in water. *J. Chem. Phys.* **2007**, *127*, 051102–1–4.

(78) Aelion, C. M.; Hohener, P.; Hunkeler, D.; Aravena, R. *Environmental Isotopes in Biodegradation and Bioremediation*; CRC Press: Boca Raton, FL, 450 p, 2010.

(79) Skell, P. S.; Hauser, C. R. The mechanism of beta-elimination with alkyl halides. *J. Am. Chem. Soc.* **1945**, *67*, 1661–1661.

(80) Zwank, L.; Elsner, M.; Aeberhard, A.; Schwarzenbach, R. P. Carbon isotope fractionation in the reductive dehalogenation of carbon tetrachloride at iron (hydr)oxide and iron sulfide minerals. *Environ. Sci. Technol.* **2005**, *39*, 5634–5641.

(81) Bernstein, A.; Shouakar-Stash, O.; Ebert, K.; Laskov, C.; Hunkeler, D.; Jeannotat, S.; Sakaguchi-Sader, K.; Laaks, J.; Jochmann, M. A.; Cretnik, S.; Jager, J.; Haderlein, S. B.; Schmidt, T. C.; Aravena, R.; Elsner, M. Compound-specific chlorine isotope analysis: A comparison of gas chromatography/isotope ratio mass spectrometry and gas chromatography/quadrupole mass spectrometry methods in an interlaboratory study. *Anal. Chem.* **2011**, *83*, 7624–7634.

(82) Sutton, N. B.; Grotenhuis, J. T. C.; Langenhoff, A. A. M.; Rijnaarts, H. H. M. Efforts to improve coupled in situ chemical oxidation with bioremediation: a review of optimization strategies. *J. Soils Sediments* **2011**, *11*, 129–140.

(83) Weathers, L. J.; Parkin, G. F.; Alvarez, P. J. Utilization of cathodic hydrogen as electron donor for chloroform cometabolism by a mixed, methanogenic culture. *Environ. Sci. Technol.* **1997**, *31*, 880–885.

(84) Novak, P.; Daniels, L.; Parkin, G. Enhanced dechlorination of carbon tetrachloride and chloroform in the presence of elemental iron

and *Methanosarcina barkeri*, *Methanosarcina thermophila*, or *Methanosaeta concillii*. *Environ. Sci. Technol.* **1998**, *32*, 1438–1443.

(85) Gregory, K. B.; Mason, M. G.; Picken, H. D.; Weathers, L. J.; Parkin, G. F. Bioaugmentation of Fe (0) for the remediation of chlorinated aliphatic hydrocarbons. *Environ. Eng. Sci.* **2000**, *17*, 169–181.

(86) Támara, M. L.; Butler, E. C. Effects of iron purity and groundwater characteristics on rates and products in the degradation of carbon tetrachloride by iron metal. *Environ. Sci. Technol.* **2004**, *38*, 1866–1876.

(87) Becker, J. G.; Freedman, D. L. Use of cyanocobalamin to enhance anaerobic biodegradation of chloroform. *Environ. Sci. Technol.* **1994**, *28*, 1942–1949.

(88) Guerrero-Barajas, C.; Field, J. A. Riboflavin- and cobalamin-mediated biodegradation of chloroform in a methanogenic consortium. *Biotechnol. Bioeng.* **2005**, *89*, 539–550.